Journal of Glaciology, Vol. 50, *No.* 169, 2004

A sedimentological and isotopic study of the origin of supraglacial debris bands: Kongsfjorden, Svalbard

Bryn HUBBARD, Neil GLASSER, Michael HAMBREY, James ETIENNE
Centre for Glaciology, Institute of Geography and Earth Sciences, University of Wales, Aberystwyth SY23 3DB, Wales
E-mail: byh@aber.ac.uk

ABSTRACT. Debris bands associated with supraglacial moraines and associated basal deposits have been logged and sampled for their ice and debris at three glaciers in northwest Spitsbergen, Svalbard. Physical properties, including sediment concentrations, sediment particle-size distributions, clast macro-fabrics, and oxygen isotope compositions, indicate that all transverse and some longitudinal debris bands originate from the basal zone of these glaciers. Transverse supraglacial bands are composed of extensive stratified-facies basal ice that is enriched in ^{18}O and which contains polymodal debris with spatially consistent clast fabrics. These properties suggest initial formation as basal ice and subsequent elevation into an englacial position by thrusting rather than formation as crevasse fills. The formation of longitudinal debris bands results from laterally compressive folding in response to the convergence of multiple flow units into a narrow glacier tongue. In common with transverse debris bands, longitudinal bands appear to be composed of stratified basal ice. The bands exposed at the surface of austre Brøggerbreen comprise two subfacies, strongly suggesting that the glacier was at least partially warm-based in the past, when the basal ice formed.

INTRODUCTION

A wide range of processes can result in the entrainment of sediment into ice masses. Supraglacial material may fall onto the ice surface and be carried with the local flow vector, leading to burial in the accumulation area and exhumation in the ablation area. Large amounts of debris can also be entrained at the glacier margins and bed. This typically occurs through a debris-rich basal ice layer, which is formed by water freezing in the presence of debris near the basal interface (e.g. Hubbard and Sharp, 1989; Alley and others, 1997; Knight, 1997). Although the mechanism remains unproven, it has been argued that basal sediments may also be incorporated into the body of a glacier through folding and thrusting (Goldthwait, 1951; Tison and others, 1989; Hambrey and others, 1999), and as basal crevasse-fills (Mickelson and Berkson, 1974; Sharp, 1985; Bennett and others, 1996; Evans and Rea, 1999; Ensminger and others, 2001; Woodward and others, 2002).

Extensive linear ridges of sediment-rich ice, commonly capped with a layer of melted-out debris, have recently been reported in the ablation area of numerous polythermal glaciers, particularly in Svalbard. These ridges are generally aligned either parallel to the ice-flow direction or perpendicular to it, and are respectively referred to hereafter as longitudinal and transverse supraglacial moraine ridges. These features are described in more detail below.

Longitudinal supraglacial moraine ridges

Longitudinal supraglacial moraine ridges, or medial moraines, located at the tongues of several composite Svalbard glaciers, have recently been interpreted by Hambrey and others (1999) and Hambrey and Glasser (2003) as products of folding along flow-parallel axes. The moraines are aligned parallel to longitudinal foliation and, with this structure, form an axial-planar relationship with the folding which develops in response to lateral compression as multiple flow units converge into a narrow tongue (Fig. 1). These authors reported that the debris-charged ridges associated with this folding emerge at the glacier surface near its terminus as fold hinges that plunge gently up-glacier.

Hambrey and Glasser (2003) reported that the debris forming supraglacial moraine ridges at vestre Lovénbreen and austre Brøggerbreen can be either coarse and angular, indicating a supraglacial origin, or (more commonly) composed of diamicton containing subrounded, faceted and striated clasts, indicating a basal origin. Orientation measurements by these authors indicated that these basally derived clasts are strongly aligned parallel to the local longitudinal foliation and associated fold axis. In such cases, it was inferred by Hambrey and others (1999) that the source material (subglacial sediment or debris-rich basal ice) is folded along flow-parallel axes directly into the body of the glacier and reaches the surface as a consequence of this folding and subsequent ablation (Fig. 1).

Transverse supraglacial moraine ridges

Glasser and others (1998) associated transverse supraglacial moraine ridges on the glaciers of Kongsfjorden with structures interpreted as thrusts. As with longitudinal moraine ridges, the visual appearance of this debris is consistent with a basal origin, but few quantitative data support this inference.

Woodward and others (2002) recently presented an alternative hypothesis for the origin of the debris bands

https://doi.org/10.3189/172756504781830114 Published online by Cambridge University Press

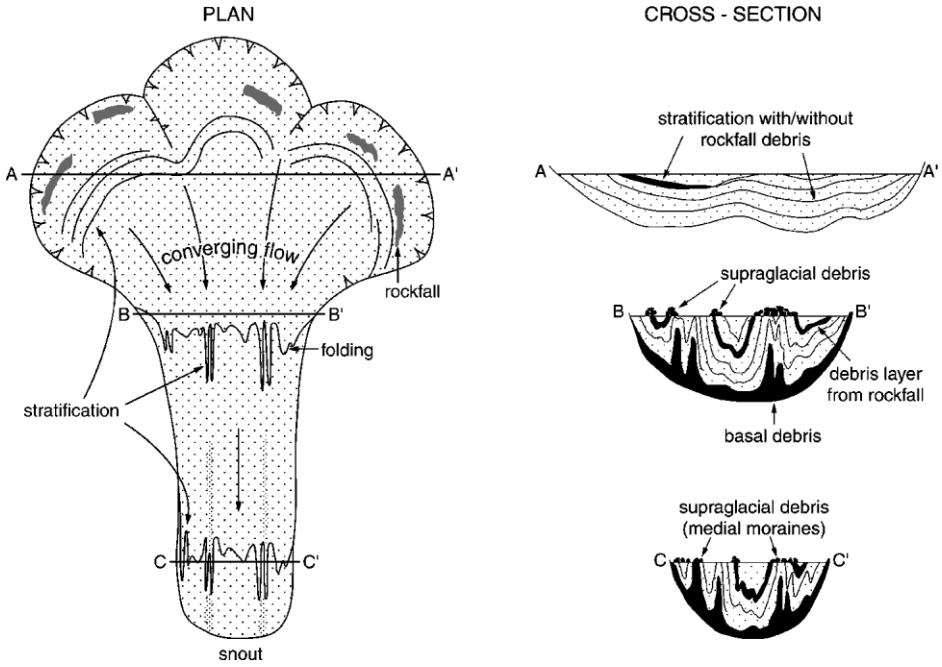

Fig. 1. Schematic illustration of the formation of longitudinal supraglacial moraine ridges at Svalbard glaciers (after Hambrey and others, 1999).

associated with transverse supraglacial moraine ridges at Kongsvegen. They argued that the features originated from debris-filled basal crevasses that have been exposed at the glacier surface by ablation of the overlying ice. However, in common with the thrust hypothesis outlined above, no new data relating to the physical properties of the materials concerned were reported.

An origin for debris bands by basal crevasse filling, however, has been advanced on the basis of research at other glaciers, from where data have been reported. Ensminger

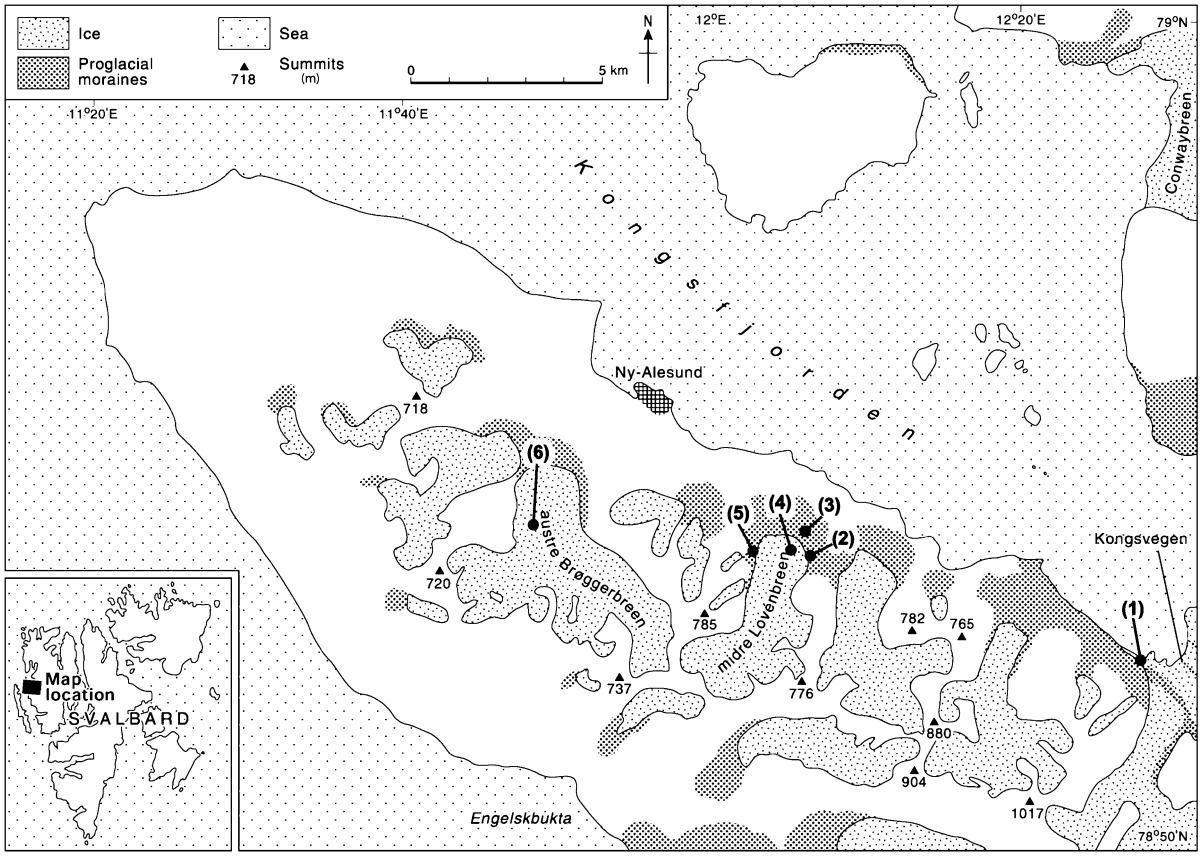

Fig. 2. Kongsfjorden with sample sites numbered: (1) Kongsvegen transverse supraglacial moraine ridge and nearby glacier margin; (2–5) midre Lovénbreen east margin (2), proglacial area (3), longitudinal supraglacial moraine ridge (4) and west margin (5); and (6) austre Brøggerbreen longitudinal supraglacial moraine ridge.

https://doi.org/10.3189/172756504781830114 Published online by Cambridge University Press

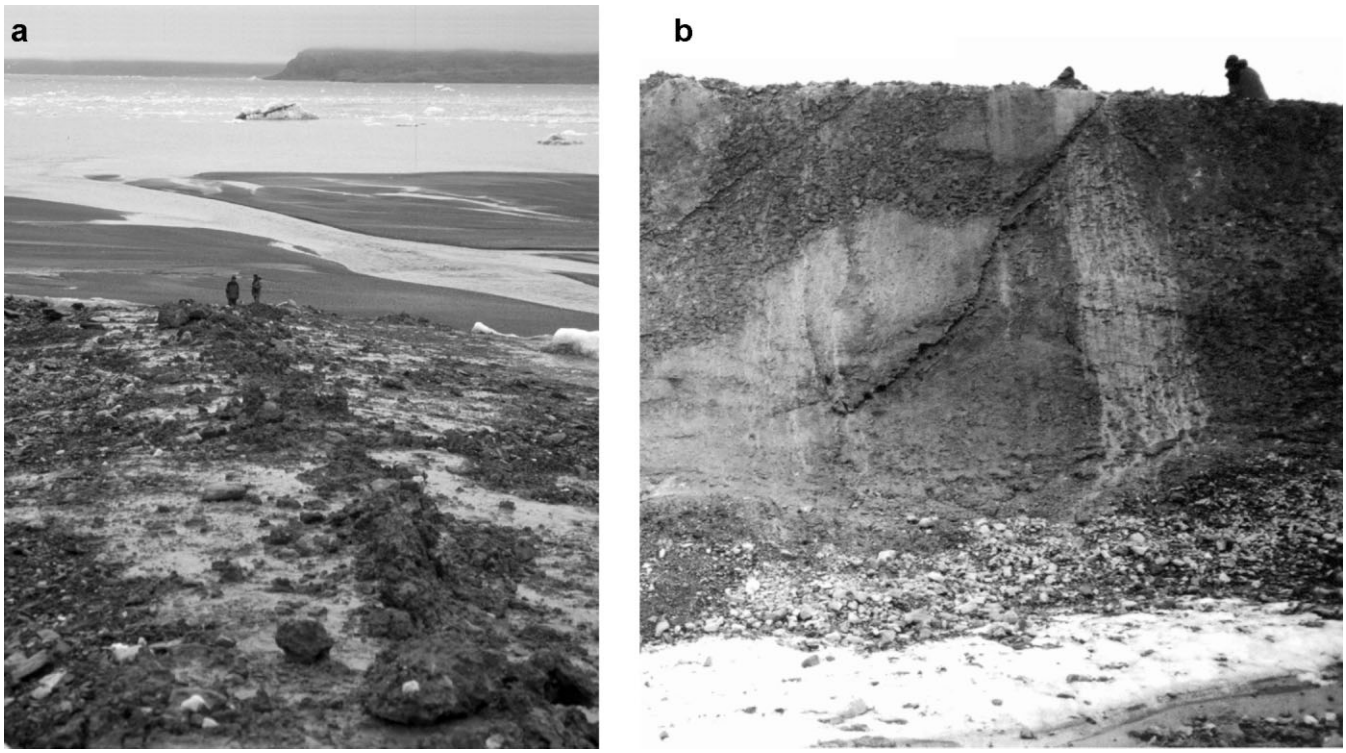

Fig. 3. Transverse moraine ridge exposed (a) on the surface of Kongsvegen (viewing towards the north) and (b) at the nearby glacier margin (viewing towards the south). Figures for scale are in roughly the same location in both photographs.

and others (2001), for example, describe a finely layered (mm thick) sequence of debris-rich and debris-poor bands interpreted to have originated as basal crevasse fills at Matanuska Glacier, Alaska, U.S.A. In this case, the layers were associated with the injection of sediment-rich water into basal crevasses, where it froze in part as a result of supercooling upon emergence from a basal overdeepening. These authors also found that the debris within these basal crevasse fills was well sorted, silt-rich and fined with distance above the bed — consistent with grain settling through a viscous suspension during formation. Not all such debris injections, however, are considered to have involved sediment-laden water. Sharp (1985), for example, argued that crevasse-squeeze ridges can form as a result of viscous soft-sediment injection into basal crevasses that open during surging. In such cases, the resulting features are more likely to include massive and poorly sorted debris, containing coarse clasts, than those associated with the less viscous flow described by Ensminger and others (2001). However, these two cases most probably represent near end-members of a range of forms whose degree of sorting and layering corresponds to the extent of fluidization experienced during formation. Sharp (1985) and Evans and Rea (1999) also point out that the character of crevasse fills may be altered after formation by, for example, ice-deformation depositional processes.

Processes of incorporation and transport may also be investigated through analysis of the fabric of the clasts present within debris bands. For example, a spatially variable, but locally strong, fabric might be anticipated within a fluidized crevasse fill, similar to a viscous debris flow (Lawson, 1979a), whereas a more extensive and consistent fabric orientation might be anticipated within a thrust or thin shear zone.

Research approach

In this study we investigate the physical properties, particularly the sedimentology and isotopic composition, of debris bands associated with longitudinal and transverse supraglacial moraine ridges at three Kongsfjorden glaciers: Kongsvegen, midre Lovénbreen and austre Brøggerbreen. In addition to characterizing these ridges, our aim is to use their physical properties to evaluate and refine theories of their formation.

Table 1. Summary of the features observed and sampled at the three glaciers studied. √ indicates that the feature was observed; S indicates that the feature was sampled for its sedimentological characteristics; I indicates that the feature was sampled for its isotopic composition

Feature	*Kongsvegen*			*Midre Lovénbreen*			*Austre Brøggerbreen*		
Transverse supraglacial moraine	√	S		√	S				
Transverse debris band	√	S	I	√	S	I			
Longitudinal supraglacial moraine				√			√		
Longitudinal debris band				√	S	I	√	S	I
Basal stratified facies	√	S	I	√	S	I			
Basal planar facies				√	S				
Glacier ice	√		I	√		I	√		I
Supraglacial meltwater	√		I	√			√		
Bulk meltwater	√			√		I	√		

https://doi.org/10.3189/172756504781830114 Published online by Cambridge University Press

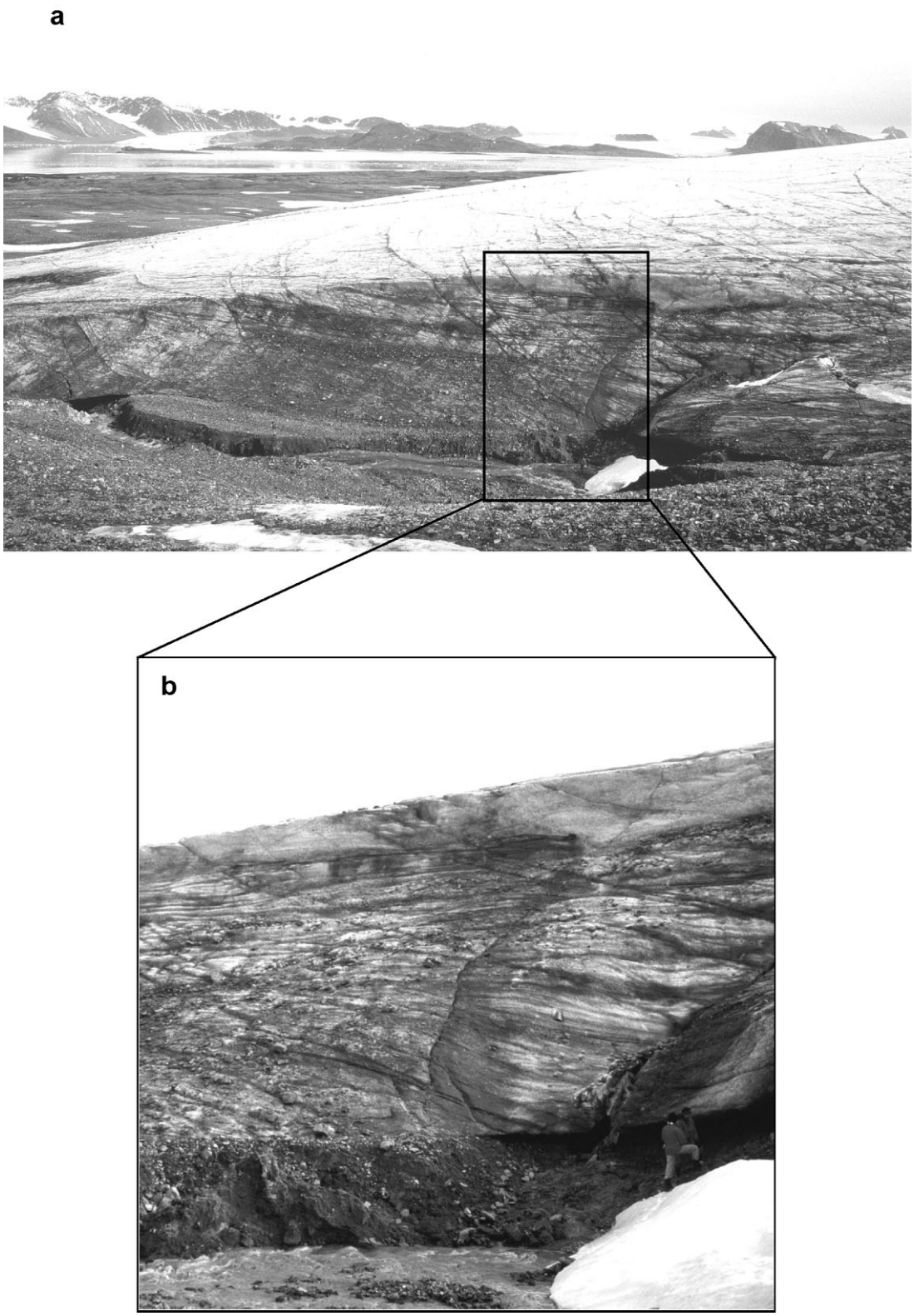

Fig. 4. West lateral margin of midre Lovénbreen: (a) general view and (b) closer view of basal solid sub-facies overlain by debris-poor, foliated glacier ice.

FIELD SITE AND METHODS

Fieldwork was undertaken at three glaciers, austre Brøggerbreen, midre Lovénbreen and Kongsvegen, located on the Brøgger peninsula (Brøggerhalvøya), Kongsfjorden, in northwest Spitsbergen, Svalbard (Fig. 2). All three glaciers have been the subject of a long-term mass-balance monitoring programme by the Norsk Polarinstitutt (e.g. Hagen and others, 1991b), revealing a general thinning and recession (Liestøl, 1988). Kongsvegen is a surge-type glacier which last advanced in 1948. Since then it has ceased to be active and, in contrast to fast-flowing ($\sim$700 m a^{-1}) Kronebreen with which it shares a common tidewater terminus, it has a maximum surface velocity of $\sim$8 m a^{-1} (Hagen and others, 1991b).

Austre Brøggerbreen and midre Lovénbreen are also

https://doi.org/10.3189/172756504781830114 Published online by Cambridge University Press

Fig. 5. Longitudinal moraine ridge emerging from the surface of midre Lovénbreen. Ice flow is directly out from the page.

slow-moving glaciers, with equilibrium-line surface velocities of only a few metres per year (Björnsson and others, 1996). Close to their neoglacial maxima around 1890 they had vertical terminal cliffs and were considered by Liestøl (1988) to be surging, an inference that is disputed by Hambrey and Glasser (2003), who cite the equivocal nature of Liestøl's (1988) evidence. However, proglacial geomorphic evidence indicates that these glaciers were more dynamic at that time (Glasser and Hambrey, 2001). Their continual recession since 1890 is a reflection of climate warming through the 20th century. All three glaciers have substantial parts of their bed at sub-freezing temperatures, particularly austre Brøggerbreen where no temperate englacial ice is evident on radar images (Macheret and Zhuravlev, 1982; Hagen and Sætrang, 1991), and borehole temperatures indicate that most of the base is cold (Hagen and Sætrang, 1991). Midre Lovénbreen has a warm-based interior and a frozen terminus region, while tidewater Kongsvegen is wet-based throughout. The sample sites referred to below are summarized in Table 1, marked in Figure 2 and illustrated in Figures 3–5.

Fig. 6. Longitudinal moraine ridge exposed at the surface of austre Brøggerbreen. Ice flow is away from the viewer.

Sample treatment and analysis

Ice, meltwater, frozen debris and unfrozen debris were

https://doi.org/10.3189/172756504781830114 Published online by Cambridge University Press

sampled. Unfrozen debris was sampled by hand trowel, stored and transported in sealed plastic bags. Samples of frozen debris and debris-rich ice were removed from the glacier and broken up by ice axe and melted in clean plastic bags. Samples of debris-poor ice were recovered by ice screw. All samples were transported in sealed plastic bags to a field laboratory where they were filtered, dried and weighed within 24 hours of sampling. When filtrate was retained for isotopic analysis at the Geophysical Isotope Laboratory, Copenhagen University, Denmark, it was stored and transported in sealed, dark-brown bottles. Meltwater sampled as liquid in the field was press-filtered prior to storage in sealed, dark-brown bottles.

Debris textures were determined in the laboratory at 1ϕ intervals, from -4ϕ to 3ϕ by dry sieving, and from 3ϕ to "finer than 10ϕ" by settling analysis (SediGraph 5100, Micromeritics). Results are presented on plots of size (ϕ) against weight (%) and as double logarithmic plots of particle diameter (d) against number of particles (N_d). The latter of these allows the degree of self-similarity (expressed as the correlation coefficient (R) of the variables) and fractal dimension (m) of the debris to be calculated. Here, a self-similar distribution will define a straight line ($R = 1.0000$) on the plot of log d against logN_d according to:

$$N_d = N_0 \left(\frac{d}{d_0} \right)^{-m} \quad (1)$$

(Hooke and Iverson, 1995), where N_0 is the number of particles of reference diameter d_0, and m, the fractal dimension, is given by the negative slope of the log–log plot. Although insensitive to minor changes in grain-size distribution (Benn and Gemmell, 2002), the value of m summarizes the ratio of smaller particles to larger particles over the size range analyzed. The analysis therefore provides a useful single-value expression for the character of an entire particle-size distribution, and thereby provides a straightforward means to compare samples. A self-similar distribution of tessellating cubes has a fractal dimension of 2.58 (Sammis and others, 1987), and samples of basally derived debris generally have fractal dimensions in the range 2.7–3.0 (e.g. Hooke and Iverson, 1995; Hubbard and others, 1996; Fischer and Hubbard, 1999; Khatwa and others, 1999).

Clast macro-fabrics were recorded in the field for samples of 50 prolate clasts, each with an a-axis/c-axis ratio of >2 (Andrews, 1970). The data are plotted on Schmidt equal-area lower-hemisphere projections, and summarized using standard eigenvector analysis.

Statistical testing of differences between sample data is based on two sample t tests (large samples) or U tests (small samples), and results are expressed as the probability (P) of differences in the data being due to chance. According to the notation used, "similar at $P > 0.1$" means that there is greater than a 10% chance of the samples being from the same parent population, and "different at $P < 0.01$" means that there is less than a 1% chance that the samples are from the same parent population.

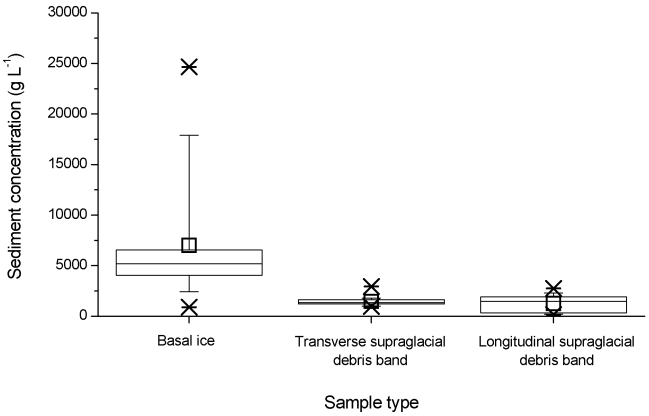

Fig. 7. Box plots of debris concentration data, classified by sample type from all three glaciers. Markers denote the 0th, 1st, 5th, 25th, 50th, 75th, 95th, 99th and 100th percentile values. The open square denotes the mean value.

RESULTS

Field sections

Transverse supraglacial moraine ridges

The transverse moraine ridge studied at Kongsvegen extended from the glacier margin for several tens of metres across the glacier surface. The surface debris formed an ice-cored mound of diamicton ~1 m high. Washing off the unconsolidated surface debris revealed a ~0.5 m wide debris band formed of thin alternating layers of debris-rich and debris-poor ice, the former containing a wide range of particle sizes. The debris-poor ice layers were largely bubble-free. Thus, it was visually similar to the stratified discontinuous sub-facies of the basal zone, as identified by Lawson (1979b) at Matanuska Glacier.

At midre Lovénbreen, a similar transverse moraine ridge extended from the glacier surface down the lateral margin, where it merged indistinctly into a layer of frozen basal sediment composed of muddy gravel. Similar to the surface debris band sampled at Kongsvegen, the band at midre Lovénbreen was formed of multiple debris-rich layers separated by relatively clean, bubble-free ice.

Table 2. Summary of sediment concentration results, classified by sample source and glacier. # indicates number of samples, $\overline{x}$ indicates the mean concentration (g L^{-1}), and σ indicates the standard deviation in concentration (g L^{-1})

Sample source	Sediment concentration (g L^{-1})											
	Kongsvegen			Midre Lovénbreen			Austre Brøggerbreen			All glaciers		
	#	$\overline{x}$	σ	#	$\overline{x}$	σ	#	$\overline{x}$	σ	#	$\overline{x}$	σ
Basal ice	2	3235	1146	11	7684	7108				13	7000	6708
Surface transverse debris bands	6	1520	725	5	1400	315				11	1466	554
Surface longitudinal debris bands							11	1259	902	11	1259	902
All debris bands										22	1362	738

https://doi.org/10.3189/172756504781830114 Published online by Cambridge University Press

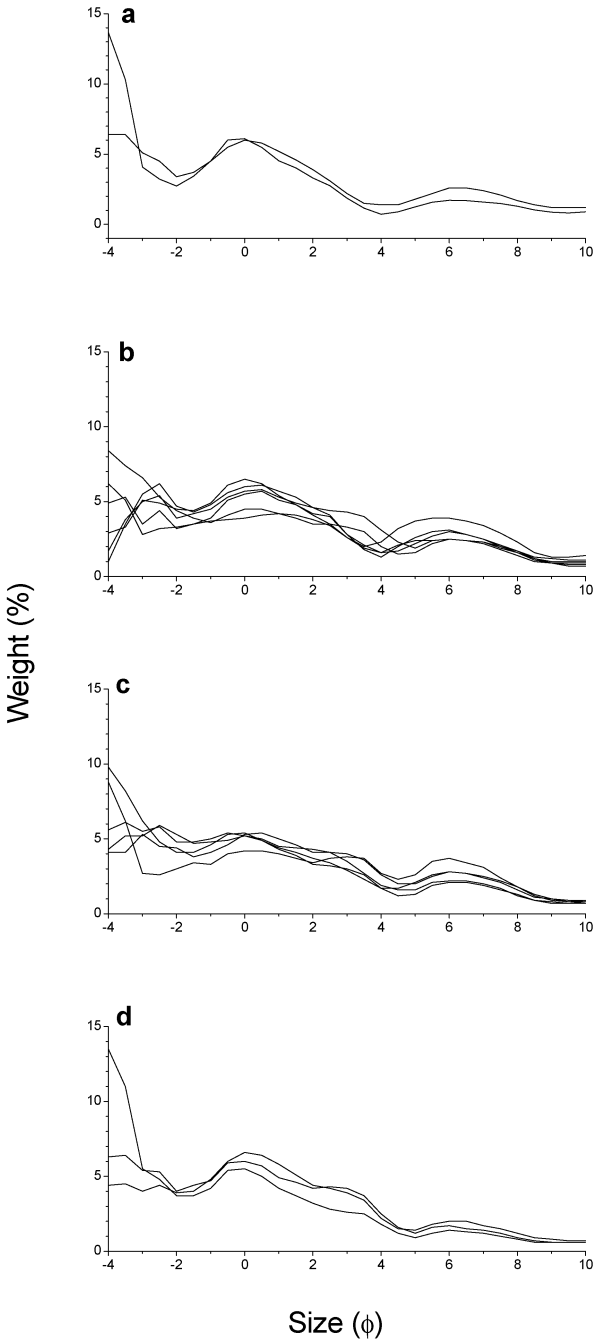

Fig. 8. Bivariate plots of weight against size class for Kongsvegen debris samples: (a) basal solid sub-facies; (b) transverse supraglacial moraine ridge; (c) ice-cliff transverse moraine ridge; (d) transverse supraglacial moraine ridge melt-out debris. The finer than 10ϕ size class is not plotted.

Longitudinal supraglacial moraine ridges

At midre Lovénbreen, the debris band associated with the longitudinal moraine studied forms part of a fold hinge that dips up-glacier at a shallow angle, consistent with Hambrey and others' (1999) structural interpretation of these features (Fig. 1). This band was layered by debris concentration, with debris-rich layers containing polymodal diamicton with clasts up to boulder size.

At austre Brøggerbreen, the debris band forming the longitudinal moraine sampled at the surface was ~50 cm thick, and close inspection revealed that it was composed of alternating debris-rich and debris-poor layers. This band was visually similar to stratified basal ice and therefore similar in structure to other debris-charged ridges sampled for the present study.

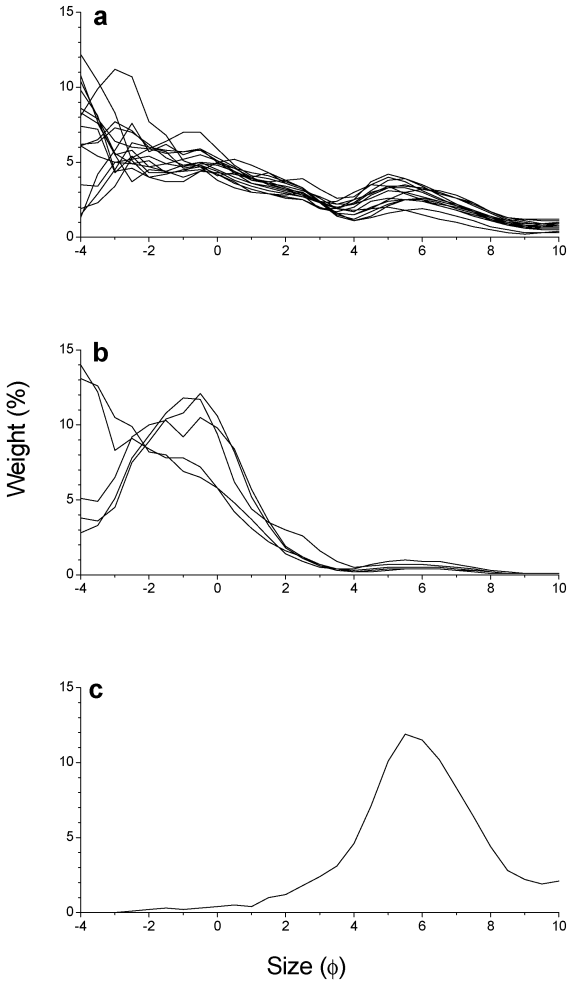

Fig. 9. Bivariate plots of weight against size class for midre Lovénbreen debris samples: (a) basal solid sub-facies; (b) transverse supraglacial moraine ridge; (c) basal planar facies. The finer than 10ϕ size class is not plotted.

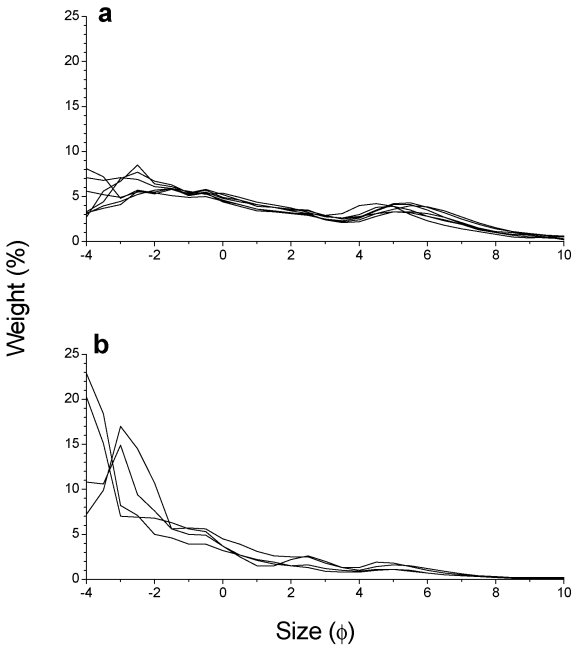

Fig. 10. Bivariate plots of weight against size class for austre Brøggerbreen debris samples: (a) longitudinal supraglacial moraine ridge (red Carboniferous debris); (b) longitudinal supraglacial moraine ridge (grey Proterozoic debris). The finer than 10ϕ size class is not plotted.

https://doi.org/10.3189/172756504781830114 Published online by Cambridge University Press

Table 3. Summary of particle-size distribution results, classified by sample source and glacier. Weight in size class (%) relates to standard size–weight plots, and m and R are the negative slope and correlation coefficient respectively of plots of log N_d against log d

Glacier	*Sample source*	*Weight in size class (%)*			*log N_d– log d*	
		Gravel	*Sand*	*Silt and clay*	*m*	*R*
All glaciers	All samples	42.9	36.7	20.4	2.76	−0.9983
Kongsvegen	All samples	36.1	42.6	21.4	2.81	−0.9993
	Basal solid sub-facies	40.5	40.0	19.6	2.80	−0.9990
	Surface transverse debris band	32.3	42.9	24.8	2.85	−0.9992
	Ice cliff transverse debris band	36.7	41.2	22.1	2.81	−0.9994
	Surface transverse debris band meltout debris	39.7	45.9	14.5	2.75	−0.9993
Midre Lovénbreen	All samples	44.4	34.5	21.2	2.76	−0.9972
	Basal solid sub-facies	42.1	34.9	23.0	2.79	−0.9992
	Surface transverse debris band	59.0	36.9	4.1	2.45	−0.9968
	Basal planar facies	0.8	16.5	82.7	3.97	−0.9733
Austre Brøggerbreen	All samples	50.1	32.0	17.9	2.69	−0.9989
	Surface longitudinal debris band (red)	39.3	36.8	23.9	2.78	−0.9988
	Surface longitudinal debris band (grey)	69.2	23.5	7.3	2.53	−0.9991

The stratified-facies ice forming the longitudinal debris band at austre Brøggerbreen was also characterized by a systematic pattern of debris incorporation. Here, thin laminae, defined by fine-grained red debris (of Carboniferous mudstone and sandstone), enveloped a core of massive, grey diamicton (of Proterozoic metamorphic rocks) containing only interstitial ice (Fig. 6). Thus, the unit incorporating the red mudstone was identical to Lawson's (1979b) stratified discontinuous sub-facies, and the unit containing the grey metamorphic material was identical to Lawson's stratified solid sub-facies. The latter is frozen debris containing interstitial ice and ice lenses.

Basal ice

Basal ice and debris were sampled from the margins of Kongsvegen and midre Lovénbreen (Table 1). In both cases the basal zone is composed of stratified-facies ice which is principally solid sub-facies. No basal ice was sampled at austre Brøggerbreen. A separate, planar, lamination some millimetres thick and containing only fine debris was also sampled at the west margin of midre Lovénbreen. This layer was parallel to the debris-charged ridge at the site and was visually similar to planar-facies basal ice identified by Hubbard and Sharp (1995) at Alpine glaciers.

Sedimentology

Debris concentration

Debris concentration (expressed as grammes of debris per litre of meltwater; $g\,L^{-1}$) was calculated for 35 samples of ice-borne debris (Table 2; Fig. 7). The mean concentration of 13 samples of basal ice sampled from ice-marginal locations is 7000 $g\,L^{-1}$, whereas that of 11 transverse and 11 longitudinal supraglacial moraine samples is 1466 and 1259 $g\,L^{-1}$ respectively. Statistical analyses of these data indicate that the supraglacial debris-band concentrations are significantly lower than the basal ice concentrations ($P < 0.01$). In contrast, the transverse and longitudinal debris-band concentrations are not significantly different from each other ($P > 0.01$).

Debris particle-size distribution

Forty-nine debris samples were analyzed for their particle-size distributions. These are classified by glacier and sample type, and plotted as size against weight in Figures 8–10. These data are also summarized in Table 3 in terms of % weight represented in the gravel (−4 to −1ϕ inclusive), sand (−0.5 to 4ϕ inclusive) and silt and clay (>4ϕ) size classes, and in terms of the correlation coefficient (R) and inverse slope (m) of bivariate plots of log number of particles against log particle diameter.

Data from Kongsvegen indicate broad similarity in the textures of the basal solid sub-facies debris, the transverse supraglacial debris band (whether sampled at the ice surface or the ice margin) and the melt-out debris forming the transverse supraglacial moraine (Fig. 8). Close inspection of Figure 8, however, indicates that the last of these has a slightly greater proportion of gravel-sized clasts (or a lower proportion of silt- and clay-sized clasts) than the debris entrained within the debris band. Analysis of these data indicates significant depletion ($P < 0.05$) of silt-sized particles in the surface moraine (14.5% silt and clay) relative to the debris bands sampled at the glacier surface (24.8% silt and clay) and margin (22.1% silt and clay). Debris entrained within the latter two sample groups is statistically similar for all three size classes ($P > 0.1$).

At midre Lovénbreen (Fig. 9) the texture of the debris within the supraglacial transverse debris band is generally similar to that of the ice-marginal basal solid sub-facies. However, in detail, the former was significantly ($P < 0.01$) depleted in silt- and clay-sized material (4.1% silt and clay) relative to both the latter (23.0% silt and clay). Both were significantly ($P < 0.01$) depleted in silt- and clay-sized material relative to the planar facies sampled at the margin of the glacier, which was very well sorted and fine-grained (82.7% silt and clay). Corresponding inverse statistical

https://doi.org/10.3189/172756504781830114 Published online by Cambridge University Press

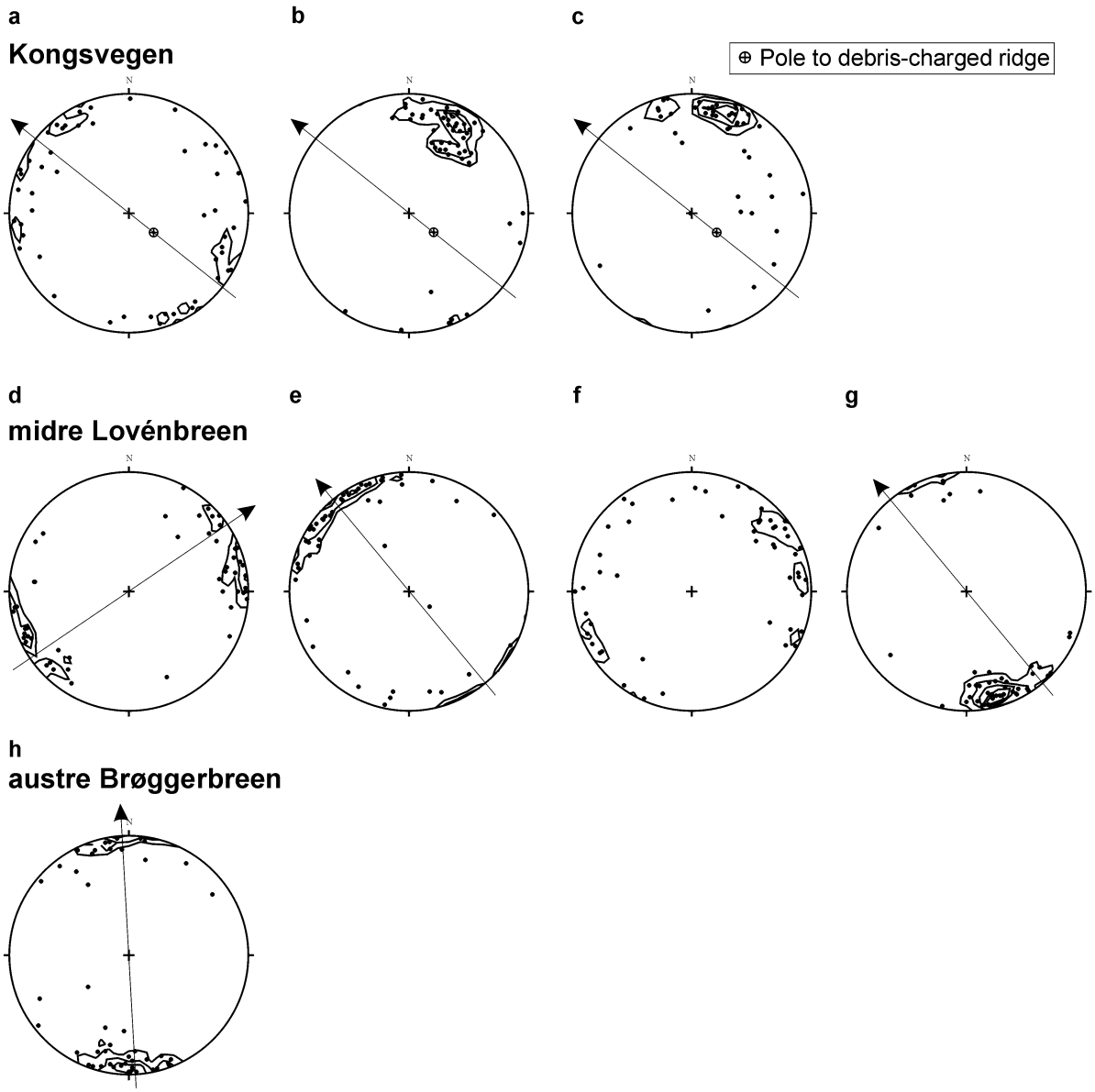

Fig. 11. Schmidt equal-area lower-hemispheric projections of clast fabric samples presented by sample type and glacier: (a) Kongsvegen basal solid sub-facies (unfrozen); (b) Kongsvegen moraine ridge from ice cliff; (c) Kongsvegen supraglacial moraine ridge; (d) midre Lovénbreen basal solid sub-facies (unfrozen) from east margin; (e) midre Lovénbreen basal solid sub-facies from west margin; (f) midre Lovénbreen proglacial diamicton (unfrozen) from east margin; (g) midre Lovénbreen basal solid sub-facies from west margin; and (h) austre Brøggerbreen supraglacial moraine ridge. Points are contoured at 5% intervals per 1% of area, and arrows indicate the local ice-flow direction.

Table 4. Summary of clast macro-fabrics as plotted on equal-area lower-hemisphere projections (Figure 11), classified by sample source and glacier

Glacier	*Sample source*	*Mean azimuth* °	*Mean dip* °	*Eigenvalues* 1st	2nd	3rd	*Sperical variance*
Kongsvegen	Basal solid sub-facies (unfrozen)	117	0	0.62	0.32	0.06	0.80
	Transverse debris band in ice cliff	23	20	0.82	0.15	0.04	0.27
	Transverse debris band on glacier surface	16	16	0.70	0.23	0.07	0.27
Midre Lovénbreen	Basal solid sub-facies (unfrozen), east margin	66	5	0.67	0.28	0.06	0.69
	Basal solid sub-facies, west margin	326	5	0.71	0.25	0.05	0.43
	Proglacial diamicton; east margin	70	1	0.80	0.14	0.06	0.77
	Basal solid sub-facies; west margin	161	8	0.88	0.09	0.03	0.31
Austre Brøggerbreen	Longitudinal debris band on glacier surface	180	4	0.83	0.13	0.05	0.64

https://doi.org/10.3189/172756504781830114 Published online by Cambridge University Press

Table 5. Summary of oxygen isotope results, classified by sample source and glacier. # indicates number of samples, $\overline{x}$ indicates the mean $\delta^{18}O$ value (standard deviation of $\delta^{18}O$ values (‰)

Glacier	*Sample source*	$\delta^{18}O$ (‰)		
		#	$\overline{x}$	σ
All glaciers	All samples	110	−11.75	0.757
Kongsvegen	All samples	39	−11.61	0.744
	Glacier ice and supraglacial meltwater	23	−12.14	0.380
	Surface transverse debris band	6	−10.82	0.294
	Ice-marginal basal ice	10	−10.85	0.399
Midre Lovénbreen	All samples	50	−11.81	0.671
	Glacier ice	21	−12.38	0.542
	Surface transverse debris band	20	−11.40	0.435
	Ice-marginal basal ice	4	−11.05	0.196
	Bulk meltwater	5	−11.66	0.048
Austre Brøggerbreen	All samples	21	−11.87	0.949
	Glacier ice	10	−11.90	1.160
	Surface longitudinal debris band (solid sub-facies)	4	−12.80	0.090
	Surface longitudinal debris band (discontinuous sub-facies)	7	−11.29	0.108

differences exist between these sample groups in the gravel-size fraction.

At austre Brøggerbreen (Fig. 10) our data indicate a marked difference between the texture of the red and the grey debris within the longitudinal supraglacial debris band. Thus, the red sediment is significantly ($P < 0.01$) depleted in gravel-sized material (39.3% gravel) and enriched in silt- and clay-sized material (23.9% silt and clay) relative to the grey sediment (69.2% gravel; 7.3% silt and clay).

Summary data of the bivariate plots of log number of particles against log particle diameter (Table 3) indicate slopes or fractal dimensions (m) that are in the range 2.6–2.9 with a few notable exceptions. The grey debris-charged ridge material at austre Brøggerbreen has a fractal dimension of 2.53, consistent with the general depletion in fines noted above. Similarly, debris sampled from the surface debris-charged ridge at midre Lovénbreen has a fractal dimension of 2.45. Conversely, the fine debris sampled from the planar facies at midre Lovénbreen has an apparent fractal dimension of 3.97, although this is questionable since the log–log bivariate plot is clearly not linear ($R = -0.973$) (Table 3).

Clast macro-fabrics

Eight sets of clast macro-fabric data were recorded from within the debris bands sampled at the three glaciers studied (Fig. 11; Table 4). At Kongsvegen the two samples recovered from the transverse supraglacial debris band (one from the marginal ice cliff and the other from the glacier surface; Table 1) are similar to each other, characterized by strong unimodal fabrics (first eigenvalues = 0.82 and 0.70) with an azimuth of ~20° and a dip of ~18°. These directions are parallel to the plan-form orientation of the supraglacial moraine and its associated debris band, i.e. transverse to the direction of ice flow. In contrast, the local ice-marginal basal diamicton is characterized by a weaker fabric (first eigenvalue = 0.62). Fabrics measured in the basal solid sub-facies located around the margins of midre Lovénbreen were also spatially variable, characterized by spherical variances of 0.67–0.88 (Table 4). At austre Brøggerbreen, the longitudinal debris-charged ridge sample from the glacier surface was characterized by a strong unimodal fabric with a first eigenvalue of 0.83.

Oxygen isotope composition

Oxygen isotope data are calculated as δ^{18}O in ‰, which expresses the ratio of the abundance of the isotope ^{18}O to ^{16}O in the sample relative to that of Standard Mean Ocean Water (SMOW):

$$\delta^{18}\mathrm{O} = 1000\left(\frac{{}^{18}\mathrm{O}/{}^{16}\mathrm{O}_{(\mathrm{sample})} - {}^{18}\mathrm{O}/{}^{16}\mathrm{O}_{(\mathrm{SMOW})}}{{}^{18}\mathrm{O}/{}^{16}\mathrm{O}_{(\mathrm{SMOW})}}\right). \quad (2)$$

Analysis of 110 ice and water samples yielded a mean value of −11.75‰ and a standard deviation of 0.76‰ (Table 5). There is little variation in the sample means between the three glaciers studied; the mean isotopic composition of ice samples was −11.61‰ ($n = 39$) from Kongsvegen, −11.81‰ ($n = 50$) from midre Lovénbreen and −11.87‰ ($n = 21$) from austre Brøggerbreen.

In order to investigate these data further, samples are subdivided by glacier and by sample type, summarized in Table 5 and Figure 12. These data reveal significant and systematic patterns in sample group isotopic composition.

At Kongsvegen, the mean composition of glacier ice and supraglacial meltwater is −12.14‰ ($n = 23$), and the mean composition of the (debris-rich) ice within the supraglacial debris band is −10.82‰ ($n = 6$). The respective values at midre Lovénbreen are −12.38‰ ($n = 21$) and −11.40‰ ($n = 20$). At both glaciers, ice within the supraglacial debris bands is isotopically enriched ($P < 0.01$) in ^{18}O relative to glacier ice and surface meltwater samples. The ice sampled from the supraglacial debris bands is isotopically similar ($P > 0.1$) to that sampled from the debris-rich basal layer (or frozen subglacial sediment) located at the margin of these glaciers: −10.85‰ ($n = 10$) at Kongsvegen and −11.05‰ ($n = 4$) at midre Lovénbreen.

At austre Brøggerbreen, the isotopic composition of the ice forming the longitudinal supraglacial debris band ($\delta^{18}\mathrm{O} = -11.83$‰; $n = 11$) is similar to ($P > 0.1$) that of glacier ice ($\delta^{18}\mathrm{O} = -11.90$‰; $n = 10$). However, if the

https://doi.org/10.3189/172756504781830114 Published online by Cambridge University Press

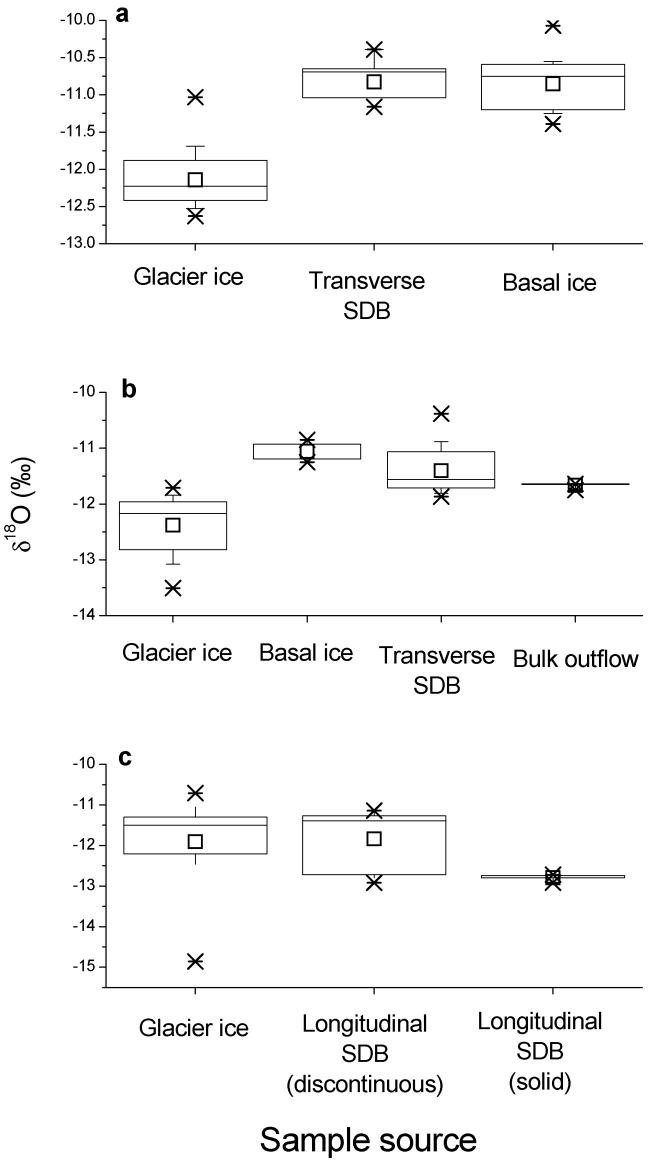

Fig. 12. Box plots of $\delta^{18}O$ composition of ice facies by sample type and glacier: (a) Kongsvegen, (b) midre Lovénbreen and (c) austre Brøggerbreen. Markers denote the 0th, 1st, 5th, 25th, 50th, 75th, 95th, 99th and 100th percentile values. The open square denotes the mean value. SDB in axis labels stands for supraglacial debris band.

samples recovered from the debris band are reclassified by sub-facies, the solid sub-facies (grey debris) is depleted in ^{18}O relative to the discontinuous sub-facies (red debris) ($P < 0.05$). Neither sub-facies has a significantly different isotopic composition from glacier ice. However, if an anomalous glacier ice sample of −14.86‰ in $\delta^{18}O$ is discounted from the analysis, the solid sub-facies becomes significantly lighter than the remaining nine glacier ice samples ($P < 0.01$).

DISCUSSION

Certain consistent relationships between the supraglacial debris bands and other sample types emerge from the evidence presented above.

Transverse supraglacial debris bands and moraine ridges

Transverse debris bands at Kongsvegen and midre Lovénbreen contain debris that is generally of similar particle-size distribution to that within basal ice at these and other glaciers (e.g. Lawson, 1979b; Hubbard and Sharp, 1995). At both Kongsvegen and midre Lovénbreen, many of the clasts entrained within the transverse debris bands are striated and faceted. They are also characterized by a strong unimodal fabric in which the clasts are aligned parallel to the plane of the supraglacial moraine ridge. At Kongsvegen, this preferred orientation is remarkably consistent at two sites, one exposed on an ice cliff and the other ~30 m distant on the glacier surface (Fig. 11b and c). At Kongsvegen and midre Lovénbreen, ice contained within the basal solid sub-facies and the supraglacial debris bands (whether at the glacier margin or glacier surface) is enriched in $\delta^{18}O$ by ~1–2 ‰ relative to local glacier ice and supraglacial meltwater. Since glacier ice (or basal meltwater derived from it) is the most likely source for the basal ice and debris-band ice, it is probable that these latter groups have been isotopically altered during their formation and/or transport. Such enrichment is consistent with open-system, or incomplete, freezing of meltwater in the presence of debris at the glacier bed (Jouzel and Souchez, 1982; Souchez and Jouzel, 1984). This is supported by the absence of any significant difference between the isotopic composition of the debris-band ice and that within the subglacial basal solid sub-facies at Kongsvegen and midre Lovénbreen.

In summary, these sedimentological data provide strong evidence that the debris incorporated within the transverse debris bands and supraglacial ridges at Kongsvegen and midre Lovénbreen was derived from the beds of these glaciers. Further, the isotopic data are consistent with the ice matrix of these debris bands also originating by refreezing at the glacier bed.

These data may also be used to shed some light on the processes responsible for forming the transverse debris bands concerned; in particular on the competing hypotheses of formation as thrusts or as basal crevasses. The main obstacle to such an interpretation is that both processes could produce features with physical and compositional similarities. Both, for example, involve the same subglacial debris and water source, and both can result in the development of strong clast fabrics within the bands they form. However, we believe the data from this study are more consistent with an origin as thrusts than with an origin as basal crevasses for the following reasons.

Fluidized flow, however viscous, of soft sediments into basal crevasses would be characterized by some degree of local debris sorting. In this study, we neither observed nor measured any such sorting. At Kongsvegen, for example, almost identical polymodal diamicton was recovered from samples of the transverse supraglacial debris band located at the glacier surface and in an ice-cliff section tens of metres distant. Although these bands were layered by variations in debris concentration, the debris was not sorted in terms of its grain-size distribution.

Fluidized flow of soft sediments into basal crevasses (at debris–water concentrations of $> 1000\ g\ L^{-1}$; Table 2) would be unlikely to result in spatially extensive, planar layering such as was observed in the present study. The transverse debris bands investigated at the surface of Kongsvegen and midre Lovénbreen were formed of extensive debris-rich layers separated by clean and

https://doi.org/10.3189/172756504781830114 Published online by Cambridge University Press

bubble-free ice, identical to stratified-facies basal ice. These properties therefore indicate that the transverse supraglacial debris bands sampled at these glaciers are formed of pre-existing stratified-facies basal ice that has been elevated from the glacier bed to the surface without noticeable alteration. While such a mechanism is incompatible with the formation of these debris bands by basal crevasse filling, it is compatible with their initial formation as basal ice and their subsequent englacial transport by thrusting.

It is likely that fluidized flow of soft sediments into basal crevasses would be characterized by some degree of fining with distance from source, as identified by Ensminger and others (2001). This effect was not observed in the present study.

Basal crevasses would be expected to cut sharply across other basal ice layers at a high angle (consistent with crevasse orientation being broadly orthogonal to the glacier bed and basal ice layers being broadly parallel to it). This effect was not observed in the present study. Conversely, we did observe continuity in the structure of individual transverse debris bands between the surface and margins of midre Lovénbreen. In this case, the bands merged indistinctly into the debris-rich basal ice layer present at the base of the lateral margin of the glacier (Fig. 4). This pattern is consistent with local ductile deformation contributing to, and occurring between, initially low-angle thrusts initiating near or at the ice–bed interface.

The heavy-isotope enrichment of the debris bands by <3 ‰ in $\delta^{18}O$ relative to glacier ice and supraglacial meltwaters is consistent with basal ice formation by open-system refreezing at the glacier bed. Indeed, such enrichment has commonly been reported in basal ice studies (Lawson and Kulla, 1978; Hubbard and Sharp, 1989). In contrast, once injected into a basal crevasse, a meltwater suspension is more likely to freeze without renewed water turnover, essentially closing the system. Sampling ice frozen in a closed system should result in a wide range of isotopic values, from slightly heavier ($\leqslant 3$ in $\delta^{18}O$) to substantially lighter (>6 ‰ in $\delta^{18}O$ as freezing nears completion) than the composition of the water in the slurry from which they formed (Jouzel and Souchez, 1982). This effect was not measured in the present study.

Although none of the individual lines of evidence presented above can be interpreted as unequivocal proof of transverse supraglacial debris-band formation as thrusting of basal ice from the glacier bed, the weight of evidence favours such a mechanism over that involving formation as sediment-filled basal crevasses. Indeed, Hubbard and Sharp (1995) interpreted planar facies basal ice sampled in the Alps as healed crevasses, probably containing aeolian debris sourced from the glacier surface. The planar facies sampled from midre Lovénbreen is similar to these features and we interpret it similarly. However, it is possible in both cases that the facies forms as a basal fracture into which fine subglacial debris may be introduced by flushing in suspension (Knight and Knight, 1994).

One further observation at Kongsvegen was that the unconsolidated material sampled from the surface of the supraglacial moraine ridge lacked fines relative to that sampled from the underlying, and ice-marginal, debris band. We interpret this effect in terms of the preferential eluviation of fine particles from surface moraine ridges by rainfall and meltwater. Similar effects were reported by Boulton and Dent (1974) and Fischer and Hubbard (1999).

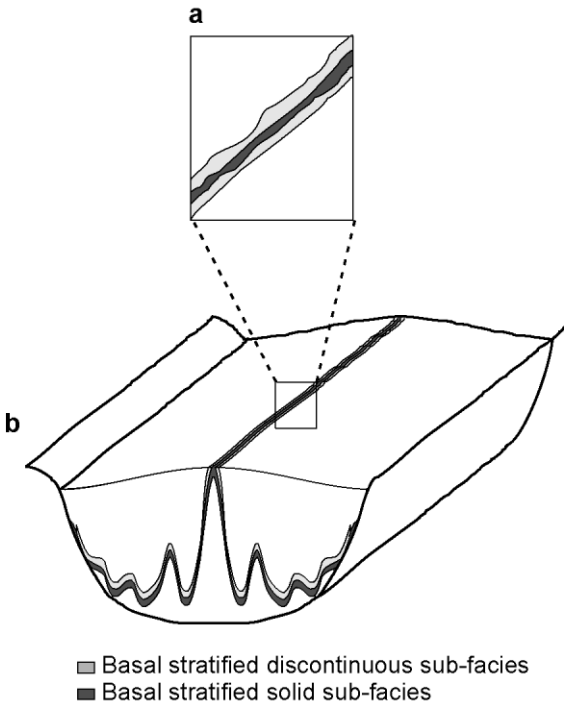

Fig. 13. Schematic illustration of the distribution of basal ice sub-facies associated with the longitudinal supraglacial moraine ridge sampled at austre Brøggerbreen (depicted in Fig. 6).

Longitudinal supraglacial debris bands and moraine ridges

The longitudinal supraglacial debris band sampled at austre Brøggerbreen contains debris that is polymodal, has a typically basal particle-size distribution and contains clasts that are faceted and striated. As with transverse debris bands at Kongsvegen and midre Lovénbreen, therefore, we interpret this material as being basally derived.

The longitudinal supraglacial debris band at austre Brøggerbreen is formed of two sub-facies: a central, solid sub-facies enveloped by a discontinuous sub-facies (Fig. 13). Associating this pattern with Hambrey and others' (1999) structural interpretation of longitudinal debris bands (Fig. 1) indicates the presence of a basal ice layer composed of two sub-facies at the bed of this glacier. Moreover, the position of the sub-facies at the surface of austre Brøggerbreen indicates that at the glacier bed the discontinuous sub-facies overlies the solid sub-facies (Fig. 13). This implies that the former was incorporated up-glacier of the latter and/or before the latter. This interpretation is consistent with the strong lithological contrast between the debris incorporated within the different sub-facies.

It is generally accepted that solid sub-facies basal ice forms by the net adfreezing of unconsolidated subglacial sediments (Hubbard and Sharp, 1989). At polythermal glaciers, this is associated with temporal variations in the position of the freezing isotherm at the boundary between subfreezing basal conditions at the ice margins and temperate basal conditions beneath thicker ice up-glacier (Weertman, 1961). In contrast, thinly layered discontinuous sub-facies

https://doi.org/10.3189/172756504781830114 Published online by Cambridge University Press

basal ice forms from repeated freezing events more likely to be associated with generally temperate basal conditions. Such freezing may involve a number of processes including: (i) the initial formation of finely laminated ice by closed-system regelation (Kamb and LaChappelle, 1963; Hubbard and Sharp, 1993, 1995), (ii) more extensive freeze-on associated with ephemeral patches of cold basal ice (Robin, 1976), or (iii) the freezing of supercooled waters emerging from basal overdeepenings (Alley and others, 1998, 1999; Lawson and others, 1998). We therefore infer from the patterns we record at austre Brøggerbreen that temperate basal conditions existed upflow of marginal freezing conditions at the time of the formation of the ice now exposed in the longitudinal debris band at the glacier's surface. Since austre Brøggerbreen is currently largely cold-based (Hagen and Sætrang, 1991; Hagen and others, 1991a), it is likely that these basal ice sub-facies formed >100 years ago, when the glaciers of the area were generally thicker and more dynamic than at present (Glasser and Hambrey, 2001).

The discontinuous sub-facies debris band is isotopically similar to glacier ice at austre Brøggerbreen, and both are isotopically heavier than the solid sub-facies debris band sampled at the glacier. The isotopic similarity of the discontinuous sub-facies to the glacier ice must be explained in the light of the size of the sample collected relative to the scale of individual freezing events (the latter being a unit of ice formed from a closed and isotopically uniform water body). Since the discontinuous sub-facies at austre Brøggerbreen contains millimeter-scale laminae, and the ice screw used to sample it was ~10 mm in diameter, no isotopic enrichment would be expected if the sub-facies formed by closed-system refreezing of water that was isotopically similar to current glacier ice (Jouzel and Souchez, 1982; Hubbard and Sharp, 1993). This and the physical structure of the discontinuous sub-facies are consistent with initial formation by Weertman regelation (Weertman, 1964), implying that the ice formed in an area of the glacier bed that was temperate and probably bedrock-based (Kamb and LaChapelle, 1963; Hubbard and Sharp, 1993).

Two interpretations may be advanced for the relative isotopic lightness (by ~1‰ in $\delta^{18}O$) of the solid sub-facies relative to glacier ice at austre Brøggerbreen. First, the sub-facies may have formed by the open-system freezing of source water that was, at the time of formation, >1 ‰ lighter in $\delta^{18}O$ than current glacier ice. Second, the sub-facies may have formed by the closed-system freezing of source water that was, at the time of formation, ~1‰ lighter in $\delta^{18}O$ than current glacier ice. In the latter case, for isotope samples to be of the restricted range in $\delta^{18}O$ measured, the scale of each freezing event would have to be smaller than our sample size (~10 mm vertically). This is unlikely given the massive and undifferentiated nature of the solid sub-facies. We therefore favour formation of the solid sub-facies ice at austre Brøggerbreen by the open-system freezing of water that was at least 1‰ lighter in $\delta^{18}O$ than current glacier ice. However, these competing hypotheses can really only be evaluated with confidence in the light of more ice and water samples from the glacier, particularly from its base.

CONCLUSIONS

Physical properties of debris bands, from which supraglacial moraine ridges are formed, suggest all transverse bands and some longitudinal bands are sourced from the glacier bed. The sedimentology and isotopic composition of transverse bands indicate formation from pre-existing basal ice that has been elevated with little bulk modification into an englacial position. Our evidence suggests the process responsible for this elevation is more likely to be related to thrusting than to the filling of basal crevasses.

Longitudinal debris bands can also be sourced from the glacier bed, and one such band was observed at austre Brøggerbreen to be formed of two distinct sub-facies. Isotopic analysis of these sub-facies indicates that the glacier was polythermal, with a temperate interior and a frozen margin, at the time of basal ice formation.

ACKNOWLEDGEMENTS

We thank T. Knudsen (University of Aarhus, Denmark) and C. Hammer (Geophysical Isotope Laboratory, Copenhagen University) for arranging the isotope sample analyses. We also thank D. Evans and D. Lawson for commenting on the manuscript, as a result of which it has been greatly improved. This work was partly funded by a U.K. Natural Environment Research Council (NERC) grant (GST022192). J.E. acknowledges funding by NERC studentship NER/S/A/2000/03690.

REFERENCES

Alley, R. B., K. M. Cuffey, E. B. Evenson, J. C. Strasser, D. E. Lawson and G. J. Larson. 1997. How glaciers entrain and transport basal sediment: physical constraints. *Quat. Sci. Rev.*, **16**(9), 1017–1038.

Alley, R. B., D. E. Lawson, E. B. Evenson, J. C. Strasser and G. J. Larson. 1998. Glaciohydraulic supercooling: a freeze-on mechanism to create stratified, debris-rich basal ice. II. Theory. *J. Glaciol.*, **44**(148), 563–569.

Alley, R. B., J. C. Strasser, D. E. Lawson, E. B. Evenson and G. J. Larson. 1999. Some glaciological and geological implications of basal-ice accretion in an overdeepening. *In* Mickelson, D. M. and J. W. Attig, *eds. Glacial processes: past and present.* Boulder, CO, Geological Society of America, 1–9. (Special Paper 337.)

Andrews, J. T. 1970. *Techniques of till fabric analysis.* Norwich, Geo Abstracts, British Geomorphological Research Group. (BGRG Technical Bulletin 6.)

Benn, D. I. and A. M. D. Gemmell. 2002. Fractal dimensions of diamictic particle-size distribution: simulations and evaluation. *Geol. Soc. Am. Bull.*, **114**(5), 528–532.

Bennett, M. R., M. J. Hambrey, D. Huddart and J. F. Ghienne. 1996. The formation of a geometrical ridge network by the surge-type glacier Kongsvegen, Svalbard. *J. Quat. Sci.*, **11**(6), 437–449.

Björnsson, H. *and 6 others.* 1996. The thermal regime of sub-polar glaciers mapped by multi-frequency radio-echo sounding. *J. Glaciol.*, **42**(140), 23–32.

Boulton, G. S. and D. L. Dent. 1974. The nature and rates of post-depositional changes in recently deposited till from south-east Iceland. *Geogr. Ann.*, **56A**(3–4), 121–134.

Ensminger, S. L., R. B. Alley, E. B. Evenson, D. E. Lawson and G. J. Larson. 2001. Basal-crevasse-fill origin of laminated debris bands at Matanuska Glacier, Alaska, U.S.A. *J. Glaciol.*, **47**(158), 412–422.

Evans, D. J. A. and B. R. Rea. 1999. Geomorphology and sedimentology of surging glaciers: a land-systems approach. *Ann. Glaciol.*, **28**, 75–82.

Fischer, U. H. and B. Hubbard. 1999. Subglacial sediment textures: character and evolution at Haut Glacier d'Arolla, Switzerland. *Ann. Glaciol.*, **28**, 241–246.

Glasser, N. F. and M. J. Hambrey. 2001. Styles of sedimentation beneath Svalbard valley glaciers under changing dynamic and thermal regimes. *J. Geol. Soc. London*, **158**(4), 697–707.

Glasser, N. F., M. J. Hambrey, K. R. Crawford, M. R. Bennett and D. Huddart. 1998. The structural glaciology of Kongsvegen, Svalbard, and its role in landform genesis. *J. Glaciol.*, **44**(146), 136–148. (Erratum: **46**(154), 2000, p. 538.)

Goldthwait, R. P. 1951. Development of end moraines in east-central Baffin Island. *J. Geol.*, **59**(6), 567–577.

Hagen, J. O. and A. Sætrang. 1991. Radio-echo soundings of sub-polar glaciers with low-frequency radar. *Polar Res.*, **9**(1), 99–107.

Hagen, J. O., O. M. Korsen and G. Vatne. 1991a. Drainage pattern in a subpolar glacier: Brøggerbreen, Svalbard. *In* Gjessing, Y., J. O. Hagen, K. A. Hassel, K. Sand and B. Wold, *eds. Arctic hydrology: present and future tasks. Hydrology of Svalbard — hydrological problems in a cold climate*. Oslo, Norwegian National Committee for Hydrology, 121–131. (Report 23.)

Hagen, J. O., B. Lefauconnier and O. Liestøl. 1991b. Glacier mass balance in Svalbard since 1912. *International Association of Hydrological Sciences Publication* 208, (Symposium at St Petersburg 1990 — *Glaciers–Ocean–Atmosphere Interactions*), 313–328.

Hambrey, M. J. and N. F. Glasser. 2003. The role of folding and foliation development in the genesis of medial moraines: examples from Svalbard glaciers. *J. Geol.*, **111**(4), 471–485.

Hambrey, M. J., M. R. Bennett, J. A. Dowdeswell, N. F. Glasser and D. Huddart. 1999. Debris entrainment and transfer in polythermal valley glaciers. *J. Glaciol.*, **45**(149), 69–86.

Hooke, R. LeB. and N. R. Iverson. 1995. Grain-size distribution in deforming subglacial tills: role of grain fracture. *Geology*, **23**(1), 57–60.

Hubbard, B. and M. Sharp. 1989. Basal ice formation and deformation: a review. *Prog. Phys. Geogr.*, **13**(4), 529–558.

Hubbard, B. and M. Sharp. 1993. Weertman regelation, multiple refreezing events and the isotopic evolution of the basal ice layer. *J. Glaciol.*, **39**(132), 275–291.

Hubbard, B. and M. Sharp. 1995. Basal ice facies and their formation in the western Alps. *Arct. Alp. Res.*, **27**(4), 301–310.

Hubbard, B., M. Sharp and W. J. Lawson. 1996. On the sedimentological character of Alpine basal ice facies. *Ann. Glaciol.*, **22**, 187–193.

Jouzel, J. and R. A. Souchez. 1982. Melting–refreezing at the glacier sole and the isotopic composition of the ice. *J. Glaciol.*, **28**(98), 35–42.

Kamb, B. and E. LaChapelle. 1963. Direct observations of the mechanism of glacier sliding over bedrock. *J. Glaciol.*, **5**(38), 159–172.

Khatwa, A., J. K. Hart and A. J. Payne. 1999. Grain textural analysis across a range of glacial facies. *Ann. Glaciol.*, **28**, 111–117.

Knight, P. G. 1997. The basal ice layer of glaciers and ice sheets. *Quat. Sci. Rev.*, **16**(9), 975–993.

Knight, P. G. and D. A. Knight. 1994. Correspondence. Glacier sliding, regelation water flow and development of basal ice. *J. Glaciol.*, **40**(136), 600–601.

Lawson, D. E. 1979a. A comparison of the pebble orientations in ice and deposits of the Matanuska Glacier, Alaska. *J. Geol.*, **87**(6), 629–645.

Lawson, D. E. 1979b. Sedimentological analysis of the western terminus region of the Matanuska Glacier, Alaska. *CRREL Rep.*, 79-9.

Lawson, D. E. and J. B. Kulla. 1978. An oxygen isotope investigation of the origin of the basal zone of the Matanuska Glacier, Alaska. *J. Geol.*, **86**(6), 673–685.

Lawson, D. E., J. C. Strasser, E. B. Evenson, R. B. Alley, G. J. Larson and S. A. Arcone. 1998. Glaciohydraulic supercooling: a freeze-on mechanism to create stratified, debris-rich basal ice. I. Field evidence. *J. Glaciol.*, **44**(148), 547–562.

Liestøl, O. 1988. The glaciers in the Kongsfjorden area, Spitsbergen. *Nor. Geogr. Tidsskr.*, **42**(4), 231–238.

Macheret, Yu. Ya. and A. B. Zhiravlev. 1982. Radio echo-sounding of Svalbard glaciers. *J. Glaciol.* **28**(99), 295–314.

Mickelson, D. M. and J. M. Berkson. 1974. Till ridges presently forming above and below sea level in Wachusett Inlet, Glacier Bay, Alaska. *Geogr. Ann.*, **56A**(1–2), 111–119.

O'Neil, J. R. 1968. Hydrogen and oxygen isotope fractionation between ice and water. *J. Phys. Chem.*, **72**(10), 3683–3684.

Robin, G. de Q. 1976. Is the basal ice of a temperate glacier at the pressure melting point? *J. Glaciol.*, **16**(74), 183–196.

Sammis, C., G. King and R. Biegel. 1987. The kinematics of gouge deformation. *Pure and Applied Geophysics* (*PAGEOPH*), **125**(5), 777–812.

Sharp, M. 1985. Crevasse-fill ridges — a landform type characteristic of surging glaciers? *Geogr. Ann.*, **67A**(3–4), 213–220.

Souchez, R. A. and J. Jouzel. 1984. On the isotopic composition in δD and δ^{18}O of water and ice during freezing. *J. Glaciol.*, **30**(106), 369–372.

Tison, J.-L., R. Souchez and R. Lorrain. 1989. On the incorporation of unconsolidated sediments in basal ice: present-day examples. *Z. Geomorphol. Suppl.*, **72**, 173–183.

Weertman, J. 1961. Mechanism for the formation of inner moraines found near the edge of cold ice caps and ice sheets. *J. Glaciol.*, **3**(30), 965–978.

Weertman, J. 1964. The theory of glacier sliding. *J. Glaciol.*, **5**(39), 287–303.

Woodward, J., T. Murray and A. McCaig. 2002. Formation and reorientation of structure in the surge-type glacier Kongsvegen, Svalbard. *J. Quat. Sci.*, **17**(3), 201–209.

MS received 31 July 2003 and accepted in revised form 4 May 2004